

Cambridge University Press

978-1-107-41393-1 - Materials Research Society Symposium Proceedings: Volume 557:
Amorphous and Heterogeneous Silicon Thin Films: Fundamentals to Devices—1999

Editors: Howard M. Branz, Robert W. Collins, Hiroaki Okamoto, Subhendu Guha
and Ruud Schropp

Excerpt

[More information](#)

Part I

Growth and Properties

Cambridge University Press

978-1-107-41393-1 - Materials Research Society Symposium Proceedings: Volume 557:
Amorphous and Heterogeneous Silicon Thin Films: Fundamentals to Devices—1999

Editors: Howard M. Branz, Robert W. Collins, Hiroaki Okamoto, Subhendu Guha
and Ruud Schropp

Excerpt

[More information](#)

Cambridge University Press

978-1-107-41393-1 - Materials Research Society Symposium Proceedings: Volume 557:

Amorphous and Heterogeneous Silicon Thin Films: Fundamentals to Devices—1999

Editors: Howard M. Branz, Robert W. Collins, Hiroaki Okamoto, Subhendu Guha

and Ruud Schropp

Excerpt

[More information](#)**THE FORMATION AND BEHAVIOR OF PARTICLES IN SILANE DISCHARGES**

Alan Gallagher*

JILA, University of Colorado and National Institute for Standards and Technology

Boulder, CO 80309-0440

ABSTRACT

Particle growth in silane RF discharges, and the incorporation of particles into hydrogenated-amorphous-silicon (a-Si:H) devices is described. These particles have a structure similar to a-Si:H, but their incorporation into the device is believed to yield harmful voids and interfaces. Measurements of particle density and growth in a silane RF plasma, for particle diameters of 8-50 nm, are described. This particle growth rate is very rapid, and decreases in density during the growth indicate a major flux of these size particles to the substrate. Particle densities are a very strong function of pressure, film growth rate and electrode gap, increasing orders of magnitude for small increases in each parameter. A full plasma-chemistry model for particle growth from SiH_m radicals and ions has been developed, and is outlined. It yields particle densities and growth rates, as a function of plasma parameters, which are in qualitative agreement with the data. It also indicates that, in addition to the diameter >2 nm particles that have been observed in films, a very large flux of Si_xH_m molecular radicals with $x \gg 1$ also incorporate into the film. It appears that these large radicals yield more than 1% of the film for typical device-deposition conditions, so this may have a serious effect on device properties.

INTRODUCTION

In silane (SiH_4) and $\text{SiH}_4\text{-H}_2$ discharges, a-Si:H film deposition is initiated by electron collisions that dissociate SiH_4 . This yields primarily neutral-radical fragments, but accompanied by a small fraction (typically 3-5%) of positive ions (cations) and a very small fraction (typically 0.5-1%) of negative ions (anions). The neutral radicals Si, SiH , SiH_2 , and H rapidly react with SiH_4 to form stable molecules or SiH_3 , while SiH_3 reacts only with the a-Si:H film. Thus, film growth is primarily due to the reactions of SiH_3 radicals with the surface. Cations that drift out of the plasma induce only a few percent of the growth, but as they typically strike the surface with energies in the 1-30 eV range, this can be important. The anions are produced in much smaller quantity, and they can not even reach the growing film due to sheath fields. Thus, for many years these were neglected as a contributor to film electronic properties. In recent years, however, it has become clear that these anions can profoundly influence the film, for they cause Si particles to grow in the plasma. Since anions (Si_xH_n^-) are trapped in the plasma, there is plenty of time for SiH_3^- - anion reactions to induce their growth, and this can lead to enormous values of x , the number of Si atoms. Once x exceeds perhaps 30, these anions are believed to be relatively spherical with a structure similar to that of the a-Si:H film; clustered Si at near-crystalline density with occasional H inside and an H terminated surface. Thus, these larger clusters are generally described as "particles," although they can also be described as Si_xH_n with charge z .

From standard "particle-in-plasma" theories, particles with $x > 200$ (radius $R_p > 1$ nm) are expected to be negatively charged, and consequently trapped in the plasma by the sheath fields.¹ (The number of negative charges increases linearly with R_p .) With gas flow, these charged particles are dragged away to the pump once they grow to 0.1-1 μm size ($x = 10^8$ - 10^{11}), and the film does not suffer. (Fig. 1 indicates the forces on negatively charged particles suspended in a rf plasma.) However, we discovered several years ago that particles of 2-15

Cambridge University Press

978-1-107-41393-1 - Materials Research Society Symposium Proceedings: Volume 557:

Amorphous and Heterogeneous Silicon Thin Films: Fundamentals to Devices—1999

Editors: Howard M. Branz, Robert W. Collins, Hiroaki Okamoto, Subhendu Guha

and Ruud Schropp

Excerpt

[More information](#)

nm radius escape the plasma and incorporate into the films in copious quantities.² These particles constituted 10^{-3} – 10^{-4} of the film volume, and their surface bonds to the surrounding film exceed the electronic defect density of a-Si:H by many orders of magnitude. Here I will report that those observations were just the tip of the iceberg; when smaller particles not visible in that experiment are included, particles probably constitute 1–10% of the film volume, and their bonds to the surrounding film are a significant fraction of all Si-Si bonds within the film. Thus, these particles have become a major concern, as it appears likely that voids and strained bonds occur at particle-film interfaces, particularly below the particles where subsequent growth cannot easily penetrate. Here I will describe what is now understood about this growth and incorporation of particles into the growing a-Si:H film, and mitigation methods that are suggested by this understanding.

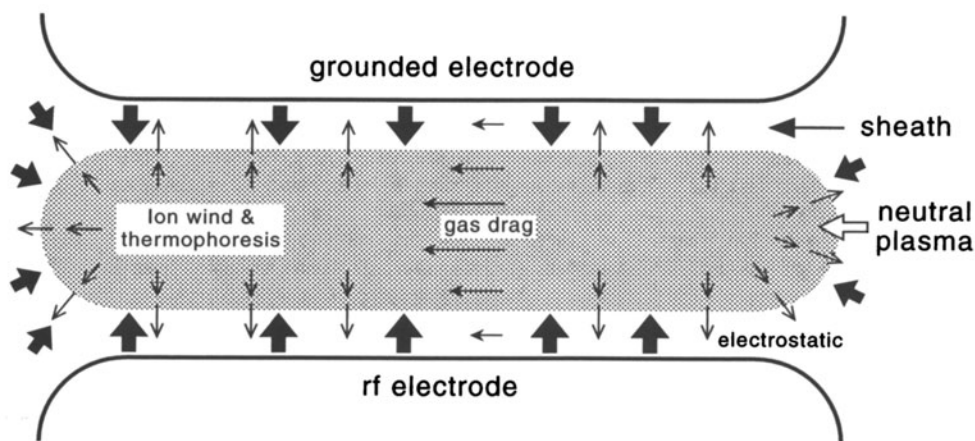


Fig. 1. Diagram of forces on negatively charged particles in a RF, capacitively coupled discharge. Electrostatic forces due to the sheath fields are indicated by large arrows, as these are the strongest forces for small particles. Ion drag results from cation-particle scattering while cations drift toward the electrodes. The gas-drag force increases as R_p^2 , whereas the other forces have slower R_p dependence. Thus, large particles are carried away to the pump.

MEASUREMENTS OF PARTICLES IN SILANE PLASMAS

Since the original detection of particles in silane plasmas by Roth et al.,³ the most common method of measuring particle suspended in plasmas is still light scattering. However, important insights have also been gained from measurements of negative ions escaping the plasma afterglow,⁴ and from scanning tunneling microscope² and transmission electron microscope (TEM) measurements of particles collected below the electrodes.⁵ Unfortunately, most of these measurements were not carried out in pure SiH_4 or $\text{SiH}_4\text{-H}_2$, or for conditions that yield device-quality a-Si:H films. Thus, to understand particle growth under device production conditions, I have utilized primarily the insights, not the particle data, from these experiments. In my laboratory we have concentrated on the conditions and gases used to produce devices, so I will primarily discuss our data. Initially, we studied the accumulation of larger particles ($R_p > 50$ nm) at the downstream end of the RF discharge, and their escape to the pumps.⁶ These particles can influence the discharge operating conditions, and their exact

Cambridge University Press

978-1-107-41393-1 - Materials Research Society Symposium Proceedings: Volume 557:

Amorphous and Heterogeneous Silicon Thin Films: Fundamentals to Devices—1999

Editors: Howard M. Branz, Robert W. Collins, Hiroaki Okamoto, Subhendu Guha

and Ruud Schropp

Excerpt

[More information](#)

location indicates an important consideration that will be discussed below in the “particle-mitigation” section: the plasma potential varies within the mid-plane between the electrodes. However, these larger particles are not suspended below the substrate and they do not incorporate into devices. Thus, in the last few years we have studied⁷ the very small particles that form directly below the substrate and are indicative of those that incorporate into films.

It is quite difficult to study the very small particles ($R_p < 20$ nm) that incorporate into films, because their light scattering cross section (Q_p), proportional to R_p^6 , is very small. Furthermore, it is not straightforward to determine the size of these very small particles, yet this must be done since the scattering signal only establishes $n_p R_p^6$ where n_p is the particle density. We have developed a method based on the particle diffusion, utilizing the fact that neutral particles diffuse out of the discharge afterglow in a time proportional to R_p^2 . An example of the scattering signal versus time is shown in Fig. 2, for a discharge that was turned on for 1.8 s. The exponential decay well after discharge termination results from fundamental-spatial-mode diffusion of 20 nm particles. With R_p thus determined, the size of the scattering signal yields n_p . This method works for $4\text{ nm} < R_p < 25\text{ nm}$, where the upper limit is due to the effect of gravity on the motion of larger particles, and the lower limit results from insufficient scattering signal.⁷

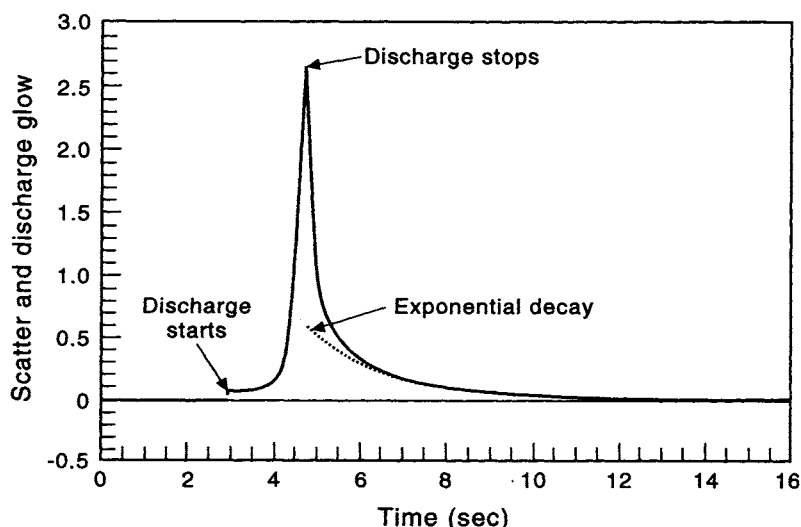


Fig. 2. Time dependence of particle scattering of a 3 W Ar^+ laser beam, for a discharge in 0.3 Torr SiH_4 that was turned on and off as indicated.⁷ The discharge RF amplitude was 82V and the film deposition rate was 0.18 nm/s.

By varying the discharge operating time, t_{on} , we measure the particle size versus discharge time, finding that R_p grows approximately linearly with time within the 4–25 nm range of the data. This can be understood from growth due to radical (primarily SiH_3) reactions on the particle surface, which is the same phenomenon that causes film growth on the substrate. In essence, for a spherical particle with silicon density ρ , $x = 4\pi R_p^3/3\rho$, $dx/dt = 4\pi R_p^2 \rho^{-1} dR_p/dt$, while the radical attachment rate dx/dt varies as the cross section πR_p^2 . The

Cambridge University Press

978-1-107-41393-1 - Materials Research Society Symposium Proceedings: Volume 557:

Amorphous and Heterogeneous Silicon Thin Films: Fundamentals to Devices—1999

Editors: Howard M. Branz, Robert W. Collins, Hiroaki Okamoto, Subhendu Guha

and Ruud Schropp

Excerpt

[More information](#)

growth is only approximately linear because the data indicates a more rapid initial growth to $R_p \approx 2$ nm, followed by essentially constant dR_p/dt . This is consistent with a small-particle cross section larger than $4\pi R_p^2$, as is expected for SiH_3 collisions with small, charged particles due to polarization forces. For a more quantitative comparison, the SiH_3 density can be established from the film growth rate, and used to calculate an expected particle growth rate due to SiH_3 collisions. The result agrees with the measurements at low pressures (P) and film growth rate (G), but the measured growth rate is as much as a factor of 2 higher than calculated at high P and G. This increased growth is tentatively attributed to heavier radicals and cations attaching to the particles, perhaps aided by an increased radical reactivity with the particle surface. This overall nearly linear growth result is thus quite reasonable, and in contrast to most previous data, demonstrating the importance of studying the low power conditions and gases appropriate for device production.

A second result is that the measured particle density decreases with discharge operating time, as the particles grow from $R_p = 4$ to 25 nm. A calculation of particle agglomeration rates demonstrates that these are orders of magnitude too small to explain this data, so particles must be escaping the plasma to the electrodes. Indeed, the escape rate implied by the data yields particle densities of $R_p = 4$ -8 nm particles in the a-Si:H film that are consistent with those measured in Ref. 2. This rate of particle escape requires that a major fraction of particles are neutral, so that they can escape the plasma. To understand how and why this happens, as well as particle formation and growth, we have developed a full plasma-chemistry model that is outlined in the next section.

A MODEL FOR PARTICLE GROWTH AND ESCAPE TO THE ELECTRODES

In this steady-state model, SiH_3 , SiH_m^+ and SiH_m^- are formed by electron collisions, typically in the ratio 100/4/0.8. These radicals grow and alter their charge due to collisions between themselves and with electrons and SiH_4 . Most of this growth results from consecutive, one-at-a-time additions of Si atoms. During this growth, the negatively charged complexes, Si_xH_m^- , are trapped in the plasma, but neutral and positively charged Si_xH_m radicals can diffuse to the electrodes. Thus, there is a continual attrition of complexes as they grow in size. When x exceeds ~ 30 and the complexes are largely cross-linked Si with a largely H-terminated surface, we think of it as a particle. The model only keeps track of x and charge z, and makes no distinction between a molecular complex and a particle, so for ease “particle” will be used to describe all Si_xH_m^z radicals or particles. With increasing x or size, particle-diffusion slows and the cross section for adding a Si atom increases. The particles can also accommodate increasing numbers of negative charge as x increases. Thus, diffusive loss is most severe for small x values, and the density of visible ($x > 10^4$) particles depends strongly on the fraction of small-x particles that are lost to diffusion before they can grow to this “large” size. The competition between growth and diffusive loss depends strongly on discharge conditions. At higher powers and pressures, the radical density is high and particle growth is rapid, while diffusion slows with increasing pressure and discharge gap (L). Thus, at high P and G many particles remain in the plasma and visible particle densities are high. On this basis, one might wish to reduce particle incorporation into films by simply lowering P and L. However, at low P and L ion bombardment of the film increases in energy, and this can also cause loss of film quality.

I will now describe the model in more detail, using the notation $n(x,z)$ for the density of particles with charge z and containing x Si atoms. The first requirement is to establish the densities $n(1,z)$ of SiH_m radicals and ions with charge $z=0,1$, and -1 . Since SiH_3 diffusing to the surface produces most of the film growth rate (G), this establishes the SiH_3 production rate

(F_0), and the density $n(1,0)$ then follows from the SiH_3 diffusion coefficient and the electrode gap. Next, based on electron collision coefficients I assume that SiH_3 , SiH_m^+ and SiH_3^- are produced in the ratio $F_0/F_1/F_{-1} = 125/5/1$. This yields $n(1,1) = F_0/R(1,1)$ and $n(1,-1) = F_{-1}/R(1,-1)$, where $R(x,z)$ is the loss rate for Si_xH_m^z , due to transforming into other x,z species and diffusion to the electrodes. Next, I calculate the particle densities $n(2,z)$ from these $n(1,z)$, based on the rate of Si atom addition from collisions with SiH_m^+ , SiH_3 and SiH_4 . Here I use available or estimated rate coefficients for collisions between these $x=1$ molecules and electrons, radicals, ions, and silane. The diffusive loss rate for these $x=1$ molecules is included in this $x=1$ to 2 step; it competes with the growth rate to $x=2$, causing some loss of $x=1$ particles. Next, this process is repeated for growth from $x=2$ to $x=3$, again with some loss of $x=2$ particles to the electrodes. This step-by-step ($x \rightarrow x+1$) particle growth is repeated to $x=10^4$ or 10^5 , a visible-particle size where comparison to experiment can be made. At appropriate x_i values where Si particles carrying $i>1$ negative charges become stable, these additional charge states are included. Iteratively calculating only $x \rightarrow x+1$ steps is an approximation, as some collisions add more than one Si atom. However, it greatly simplifies the calculation and is justified because particle growth is dominated by collisions with SiH_4 for $x<100$, and by collisions with SiH_3 for $x>100$. An example result from the calculation is shown in Fig.3 for discharge conditions that are typical of those in Ref. 7.

In Fig. 3, first consider the neutral particles that are labeled $n(z=0)$ and $\text{flux}(0)$, equivalent to $n(x,z=0)$ and $F(x,0)$ in the more general notation for particle density and flux to

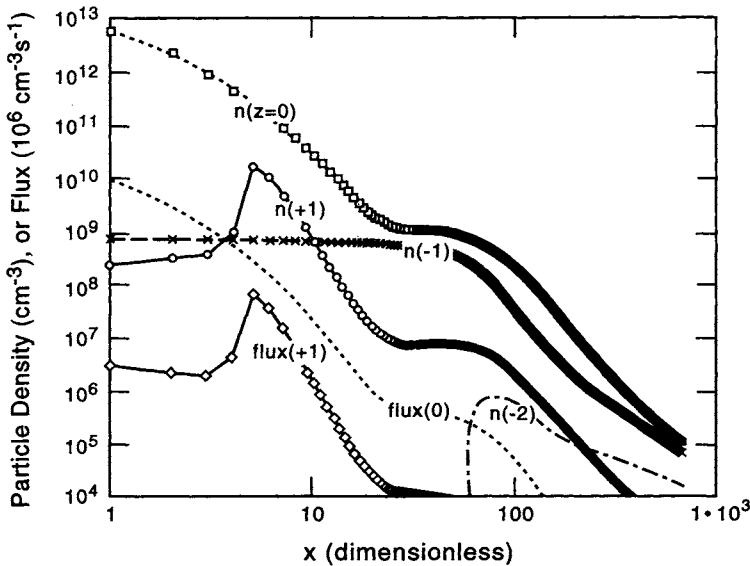


Fig. 3. Densities of particles containing x Si atoms and z charges, and flux of $z=0$ and $+1$ particles to the electrodes, in units of $10^6/\text{s}$ and cm^3 of plasma volume. The RF plasma conditions are 0.3 Torr pure SiH_4 , $T=300\text{K}$, 0.3 nm/s film growth rate, and 1.3 cm electrode gap, as in Ref. 7. To simplify the figure only the $x=1$ to 730 range is shown here; for $x>730$, particles with $z=-3$ also occur. The charged particle densities are $n_e = 3 \times 10^8 \text{ cm}^{-3}$, $n_+ = n_- = 3.6 \times 10^{10} \text{ cm}^{-3}$.

Cambridge University Press

978-1-107-41393-1 - Materials Research Society Symposium Proceedings: Volume 557:

Amorphous and Heterogeneous Silicon Thin Films: Fundamentals to Devices—1999

Editors: Howard M. Branz, Robert W. Collins, Hiroaki Okamoto, Subhendu Guha

and Ruud Schropp

Excerpt

[More information](#)

the surfaces with any charge z . These neutral particles are molecular radicals, with $x=1$ representing SiH_3 . The $x=2$ radicals result from collisions between a pair of SiH_3 , and the $x=3$ primarily result from collisions between $x=1$ and $x=2$ radicals. As x increases from 1 to 2, $n(x, z=0)$ and $F(x, 0)$ drop a factor of ~ 2.5 and ~ 3.5 respectively. As x further increases, a smaller decrease per $x \rightarrow x+1$ step occurs, due to an increase in the rates of growth/diffusive loss. (Collision cross sections increase with x , and this increases growth rates and decreases diffusion rates.) The $x < 20$ data in Fig. 3 can be approximated as $F(x, 0) \propto x^{-3}$. If one assumes that x Si atoms are incorporated into the film by each Si_xH_m radical that escapes the plasma, then 50 % of the film results from $x > 1$ radicals, 33% from $x > 2$ radicals, etc. This result involves assumed radical-radical reaction cross sections for $x > 2$, but it is unlikely that these are far off as these are highly exothermic reactions that are stabilized by H release. Thus, even before considering the larger particles, this heavy-radical incorporation could have significant effects on film properties. (This has been pointed out and modeled previously.⁸) This rate of $F(x, 0)$ falloff versus x is very sensitive to plasma parameters; it slows if G , L or P is increased and visa versa. For $x > 20$, $n(x, 0)$ begins to follow the negative ion density, $n(x, -1)$, as these populations become strongly coupled by electron and cation collisions. Since the negative ions grow rapidly for $x < 50$, both populations falloff very slowly in the $x=20-50$ range. For $x > 50$ this negative ion growth rate decreases, and diffusive loss of neutral particles again causes $n(x, 0) \propto x^{-n}$ with $n=3-4$.

Turning now to the anions, labeled $n(-1)$ in Fig.3, their density is almost independent of x for $x < 50$ due to very rapid growth and only minor loss by cation collisions. Reactions with silane cause this rapid growth, in a process that has been observed⁴ to occur for $x < \sim 30$. The measurements do not extend past $x \approx 30$, and are also somewhat ambiguous for $x > 6$, but it is clear that at some x value (x_c) the presence of a negative charge can no longer cause a reaction that does not occur on a neutral a-Si:H surface. We guess that this transition occurs when the polarization energy at the surface equals the thermal energy, yielding $x_c \approx 50$. We make x_c an adjustable parameter in the model, while $x_c = 50$ was used for the calculation of Fig. 3. As already noted, for $x > 100$ or actually $x \gg x_c$, this anion growth rate slows and diffusive loss of neutral particles causes the coupled densities of $z=0$ and -1 particles to decrease. Due to the much larger ratio of (growth rate)/(diffusion rate) in this $x > 100$ region, the attrition per $x \rightarrow x+1$ step is much smaller than in the $x=1-20$ region discussed in the previous paragraph. However, there are many more steps for $x > 100$ in Fig. 3, a fact that tends to be hidden by the $\log(x)$ scale used in the plot.

Considering next the cations, labeled $n(+1)$ and $\text{flux}(+1)$ in Fig. 3, the density of $x=1-3$ is severely lowered by very rapid growth reactions with SiH_4 . However, these reactions slow at $x=3$ and essentially terminate by $x=6$, and only slower reactions with radicals cause further cation growth. The result is a peak in $n(x, 1)$ at $x=5$, followed by a drop off to $x=20$ as cation diffusive loss competes with growth. For $x > 30$, the cations also become closely connected to the $z=-1$ and 0 particles by charge-changing collisions, and all three densities fall together. Note that, for all x values, the cation flux to surfaces is always much smaller than the neutral flux. The cation-silane reaction rates for $x < 8$, which lead to this $x=5$ peak in the $F(x, 1)$ flux, are measured values⁹ that inevitably yield this peak at $x=5 \& 6$. However, this is in severe contradiction with mass-spectrometer measurements through the substrate electrode of silane RF discharges.^{4,10} Those experiments typically observed $F(x+1, 1)/F(x, 1)$ ratios of $\sim 1/3$ for the entire $x=1-6$ range; the opposite of an increase with increasing x . The most likely explanation for this discrepancy is that the larger- x ions exist in the neutral plasma region, but breakup while traversing the sheath due to energetic collisions with SiH_4 . This is indirectly supported by comparing mass spectrometer observations from our laboratory, taken at the side of the

neutral plasma region and through the cathode of a silane discharge.¹¹ Although these measurements were in a dc discharge, we measured for $x=1-6$, $F(x,1)=\text{constant}$ when sampling at the plasma, but $F(x+1,1)/F(x,1)\approx 1/4$ through the cathode.

There is one additional trace in Fig. 3, corresponding to particles carrying two negative charges. We calculate that this becomes possible at $x=60$, so $n(x,-2)$ appears for $x>60$. As can be seen, it plays a minor role for these conditions and range of x values. This, as well as the fact that $n(x,0)/n(x,1)>1$ for $x>100$ in Fig. 3, is due to $n_+ > n_e$, where n_+ is the total cation density and n_e the electron density. This is a neutral plasma, but a charge $n_+ > n_e$ is carried by the negatively-charged particles, mostly by the anions with $x<50$ in Fig. 3. The ratio $n(x,0)/n(x,-1)$ is set by a balance between electron attachment to $n(x,0)$ and cation attachment to $n(x,-1)$, so it is a strong function of n_+/n_e . If $n_+/n_e \approx 1$, as in plasmas without negative ions, this balance would yield $n(x,0)/n(x,-1) < 1$ because electron velocities are much higher than cation velocities. This has a major effect on particle loss to the electrodes, because for each x only the neutral and positive particles can escape. Thus, the large fraction of particles that are neutral in Fig. 3 yields a very large loss flux to the electrodes. This unusually large neutral fraction results from $n_+/n_e \approx 100$ for this plasma.

Figure 4 again shows particle densities and (total) flux to the electrodes for the plasma conditions of Fig. 3. The x range is extended to 10^4 ($R_p = 3.6$ nm), higher charge states are included, and the total density is also plotted as a density of particles per nm of radius. (All other densities are per unit x .) Charge states -5 and -6 also occur in this x range, but are unimportant for these conditions and are not plotted. Note that the particle density per nm of radius is approaching a constant at large x . This is the steady-state result of a constant dR_p/dt growth rate, which occurs as described below Fig. 2 when diffusive loss is minor compared to growth. Very large particles thereby accumulate in this homogeneous plasma model, whereas

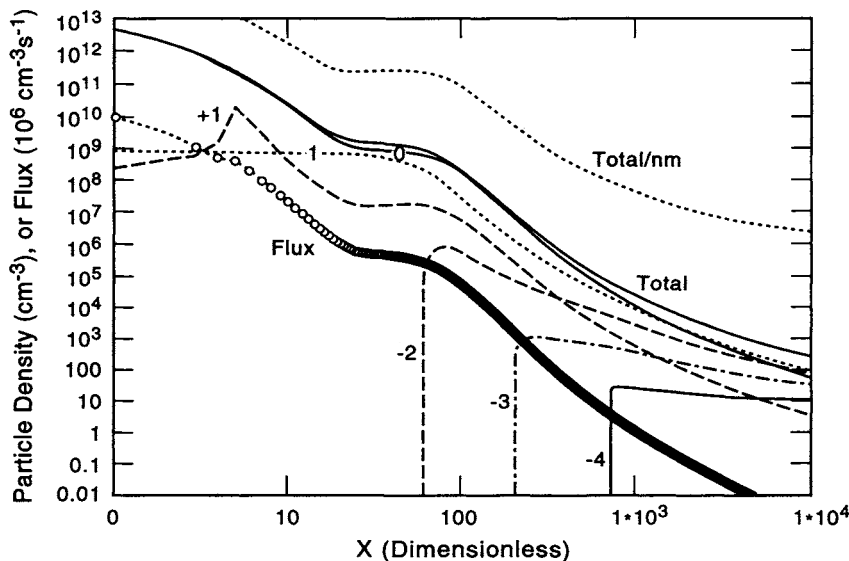


Fig. 4. Calculated particle densities, $n(x,2)$, as a function of x , the number of Si atoms, and 2, the charge. Also shown is density per nm of particle radius and particle flux to surfaces.

in the flowing-gas plasmas used to produce devices these would be normally be carried to the downstream end. However, particles may trap and grow to large size above irregularities in the electrode surfaces, since these can produce a local maxima of the plasma potential that traps negative particles. To estimate the particle sizes that occur below substrates without such irregularities, the typical measured R_p growth rates from the experiment described above should be multiplied by gas dwell times in the reactor. This might typically yield 10nm/s times 0.5s = 5 nm for a device reactor.

The particle density at $x > 10^4$ is a very sensitive function of P, G , and L . This is shown in Fig. 5, where n_4 , the total particle density per nm of radius at $x = 10^4$, is plotted. Here I have used one set of assumed collisional rate coefficients and, as almost all of these are must be estimated from chemical and physical principles, this is not a definitive result. However, the trends seen in Fig. 5 are followed for many different sets of rate coefficients, and I believe it is realistic. The n_4 density tends to limit out at 10^{10} - 10^{11} cm⁻³ nm⁻¹, which corresponds to about n_+ , the total cation charge. Since the total particle negative charge cannot exceed the cation density, most particles become neutral once the particle density exceeds n_+ . Particles then escape the plasma with a high probability, so this sets a limit on total particle density. The data is plotted versus $P \cdot L^{1.8}$ because it is found that this reduces results at different P and L values to a relatively common curve. For each G value, as $P \cdot L^{1.8}$ is reduced n_4 decreases by many orders of magnitude, and at the left side of each curve n_4 varies more than 5 orders of magnitude for a factor of 2 in this parameter or in G . This extreme sensitivity to the plasma parameters results from the multiple-step particle growth, with diffusive loss competing with growth at each step. It is consistent with the results of the experiment described above, as is the range of P, L and G that yield the measured particle densities. However, the exact values of P, L and G for which the model yields these densities is not meaningful, as many collisional rates must be assumed. It is interesting that the sensitivity to L is much stronger than to P .

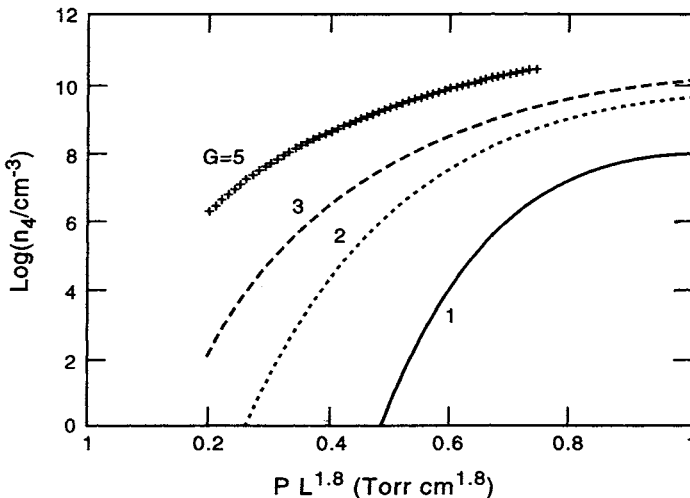


Fig. 5. $\text{Log}_{10}(n_4/\text{cm}^{-3})$ as a function of RF discharge parameters. G =film growth rate in Å/s, L = electrode gap in cm, P = silane pressure in Torr at 300 K, and n_4 is the density of 3.6 nm radius ($x=10^4$) particles per nm of radius.